HHS Public Access

Author manuscript

J Neurochem. Author manuscript; available in PMC 2015 April 22.

Published in final edited form as:

J Neurochem. 2008 October ; 107(2): 466–477. doi:10.1111/j.1471-4159.2008.05618.x.

Soluble Aggregates of the Amyloid-β Protein Selectively Stimulate Permeability in Human Brain Microvascular Endothelial Monolayers

Francisco J. Gonzalez-Velasquez, **Joseph A. Kotarek**, and **Melissa A. Moss***

Department of Chemical Engineering, University of South Carolina, 2C02 Swearingen Engineering Center, Columbia, South Carolina, 29208

Abstract

Cerebral amyloid angiopathy associated with Alzheimer's disease is characterized by cerebrovascular deposition of the amyloid-β protein (Aβ). Aβ elicits a number of morphological and biochemical alterations in the cerebral microvasculature, which culminate in hemorrhagic stroke. Among these changes, compromise of the blood-brain barrier has been described in Alzheimer's disease brain, transgenic animal models of Alzheimer's disease, and cell culture experiments. In the current study, presented data illustrates that isolated soluble $A\beta_{1\text{-}40}$ aggregates, but not unaggregated monomer or mature fibril, enhance permeability in human brain microvascular endothelial monolayers. $A\beta_{1\text{-}40}$-induced changes in permeability are paralleled by both a decrease in transendothelial electrical resistance and a re-localization of the tight junction associated protein zonula occludin-1 away from cell borders and into the cytoplasm. Small soluble $A\beta_{1\text{-}40}$ aggregates are confirmed to be the most potent stimulators of endothelial monolayer permeability by establishing an inverse relationship between average aggregate size and stimulated changes in diffusional permeability coefficients. These results support previous findings demonstrating that small soluble $A\beta_{1\text{-}40}$ aggregates are also primarily responsible for endothelial activation, suggesting that these same species may elicit other changes in the cerebrovasculature associated with cerebral amyloid angiopathy and Alzheimer's disease.

Keywords

Alzheimer's disease; amyloid-β protein; blood-brain barrier; cerebral amyloid angiopathy; permeability; soluble aggregates

Introduction

Cerebral amyloid angiopathy (CAA) is characterized by deposition of the fibrillar form of amyloidogenic proteins along perivascular drainage pathways within the cerebrovasculature, beginning in the basement membrane of larger, brain-supplying arteries and progressing into arterioles and capillaries (Kalaria 1992; Rensink *et al.* 2003; Kumar-Singh 2008; Weller *et al.* 2008). CAA exhibits a high prevalence among the elderly, affecting up to 50% of elderly

*Address correspondence to: Melissa A. Moss, Department of Chemical Engineering, University of South Carolina, 2C02 Swearingen Engineering Center, Columbia, SC 29208, Telephone: 803-777-5604, Fax: 803-777-0973, mossme@engr.sc.edu.

individuals (Rensink *et al.* 2003; Maia *et al.* 2007), and incidence increases with age (Maia *et al.* 2007). Among patients diagnosed with Alzheimer's disease (AD), the incidence of CAA rises to 80–90% (Jellinger 2002; Rensink *et al.* 2003). In AD, the amyloidogenic protein deposited within CAA lesions is the same amyloid-β protein (Aβ) that comprises the hallmark amyloid plaques found within the brain parenchyma. However, unlike parenchymal amyloid plaques, which are composed primarily of the longer, 42-residue form of Aβ, cerebrovascular plaques predominantly contain the shorter form of this protein, $A\beta_{1\text{-}40}$ (Rensink *et al.* 2003; Maia *et al.* 2007; Kumar-Singh 2008; Weller *et al.* 2008).

CAA most commonly manifests clinically as intracerebral or lobar hemorrhages (Jellinger 2002; Rensink *et al.* 2003; Maia *et al.* 2007; Kumar-Singh 2008). Several morphological and biochemical alterations in the cerebral microvasculature precede hemorrhage, including compromise of the blood-brain barrier (BBB) (Kalaria 1992; Jellinger 2002; Kumar-Singh 2008). Capillary integrity, whereby solute exchange between blood plasma and brain interstitial fluid is prevented so that molecular transport can be tightly regulated, is important for the normal functioning of the brain. This barrier is maintained in part by the presence of tight junctions (TJs) that restrict paracellular flux between brain microvessel endothelial cells (Kniesel and Wolburg 2000; Ballabh *et al.* 2004; Zlokovic 2005; Forster 2008).

Compromise of the BBB in CAA and AD is suggested by the detection of blood plasma proteins associated with amyloid plaques (Kalaria *et al.* 1991; Akiyama *et al.* 1992; Kimura *et al.* 1994; Perlmutter *et al.* 1995; Wisniewski *et al.* 1997) and within AD brain parenchyma (Vinters 1987; Kalaria 1992; Wisniewski *et al.* 1997; Zipser *et al.* 2007) at concentrations correlating positively with disease severity (Zipser *et al.* 2007). In addition, increases in microvascular permeability associated with cerebrovascular Aβ deposits (Wisniewski *et al.* 1997) and the disruption of cerebral microvasculature endothelial TJs (Claudio 1996) have been directly observed in AD brain. These *in vivo* observations are substantiated by cell culture studies. $A\beta_{25\text{-}35}$ and $A\beta_{1\text{-}40}$ increase endothelial monolayer permeability in a dose-dependent manner for cultures of porcine pulmonary artery endothelial cells (Blanc *et al.* 1997) and bovine brain capillary endothelial cells (Strazielle *et al.* 2000), respectively. Furthermore, when monolayers of rat brain microvascular endothelial cells are exposed to $A\beta_{1\text{-}42}$, endothelial TJ proteins exhibit altered expression and translocation from the cell surface to the cytoplasm (Marco and Skaper 2006).

In animal models, intracarotid infusion of $A\beta_{1\text{-}40}$, $A\beta_{1\text{-}42}$, or $A\beta_{25\text{-}35}$ induces a pronounced accumulation of plasma proteins outside the cerebral vasculature (Jancso *et al.* 1998; Su *et al.* 1999; Farkas *et al.* 2003) as well as a reduction in endothelial TJs (Farkas *et al.* 2003). Similarly, transgenic animal models of AD display an impaired BBB integrity (Ujiie *et al.* 2003; Dickstein *et al.* 2006) which correlates with age (Ujiie *et al.* 2003). Restoration of BBB integrity following the removal of Aβ deposits via immunization implicates a direct role for Aβ in this vascular deficiency (Dickstein *et al.* 2006). However, detection of BBB compromise prior to the appearance of amyloid plaque deposition (Ujiie *et al.* 2003) may suggest that Aβ aggregation species that are present prior to the appearance mature fibrils are involved in BBB deterioration.

Recently, our lab has demonstrated that isolated soluble $A\beta_{1-40}$ aggregates selectively stimulate endothelial monolayers for both adhesion and subsequent transmigration of monocyte cells and that smaller soluble aggregates are primarily responsible for endothelial activation (Gonzalez-Velasquez and Moss 2008). These findings contribute to the accumulating evidence that soluble Aβ aggregation intermediates, including Aβ-derived diffusible ligands (ADDLs), oligomers, and protofibrils, play a significant role in the pathology of AD. In the current study, the ability of small, soluble $A\beta_{1-40}$ aggregates to selectively induce endothelial monolayer permeability is investigated in a human brain microvascular endothelial cell (HBMVEC) model. By isolating $A\beta_{1-40}$ monomer, fibril, and soluble aggregates using size exclusion chromatography (SEC) and further characterizing the size of soluble aggregates via dynamic light scattering (DLS), evidence is provided that $A\beta_{1-40}$ monomer and fibril are inactive, while soluble $A\beta_{1-40}$ aggregates increase endothelial monolayer permeability, with smaller soluble aggregates exhibiting the most pronounced effect. Observed changes in permeability are accompanied by both a decrease in transendothelial electrical resistance (TEER) and a redistribution of the endothelial TJ-associated protein zonula occludin-1 (ZO-1), further substantiating the ability of soluble $A\beta_{1-40}$ aggregates to disrupt BBB integrity.

Materials and methods

Materials

$A\beta_{1-40}$ peptide was purchased from AnaSpec (San Jose, CA) or W.M. Keck Biotechnology Resource Laboratory at Yale University (New Haven, CT). Fluorescein isothiocyanate-labeled bovine serum albumin (FITC-BSA), thioflavin T, sodium bicarbonate, penicillin, streptomycin, glycine, hydrocortisone, gelatin, Dulbecco's phosphate buffered saline (D-PBS), Triton X-100, and 1,4-diazabicyclo[2.2.2]octane (DABCO) were obtained from Sigma (St. Louis, MO). BSA was obtained from EMD Chemicals (Gibbstown, NJ). CS-C Complete Medium, CS-C Serum Free Medium, CS-C Passage Reagents, and CS-C Attachment Factor were obtained from Cell Systems (Kirkland, WA). Collagen was obtained from PureCol INAMED (Fremont, CA). Recombinant human tumor necrosis factor-α (TNF-α) was purchased from Promega (Madison, WI). Paraformaldehyde was obtained form Fisher (Fair Lawn, NJ). Rabbit polyclonal anti-ZO-1 antibody was purchased from Zymed (Carlsbad, CA), and rabbit polyclonal anti-smooth muscle α-actin antibody was purchased from abcam (Cambridge, MA). Donkey normal serum and Cy3-conjugated donkey anti-rabbit antibody were purchased from Jackson Immunoresearch (West Grove, PA). 4′,6′-diamidino-2-phenylindole dihydrochloride (DAPI) was obtained from Invitrogen (Eugene, OR).

Preparation of $A\beta_{1-40}$ monomer, fibril, and soluble aggregates

Lyophilized $A\beta_{1-40}$ peptide was stored desiccated at −20°C until reconstitution and preparation as described previously (Gonzalez-Velasquez and Moss 2008). Briefly, $A\beta_{1-40}$ peptide was reconstituted in 50 mmol/L NaOH at a concentration of 2 mg/mL and pre-existing aggregates were removed by SEC on a Superdex 75 HR10/30 column (GE Healthcare, Piscataway, NJ). Isolated $A\beta_{1-40}$ monomer was used fresh or stored at 4°C for up to 24 h.

Fibrils and soluble aggregates were prepared from isolated monomeric $A\beta_{1\text{-}40}$ as described previously (Gonzalez-Velasquez and Moss 2008). Briefly, monomeric $A\beta_{1\text{-}40}$ (100–200 μmol/L) was agitated vigorously at room temperature in the presence of 2–250 mmol/L NaCl and 40 mmol/L Tris-HCl (pH 8.0) for 4–20 h and aggregation was monitored by thioflavin T fluorescence using an LS-45 luminescence spectrometer (Perkin-Elmer, Walthan, MA). Unpurified $A\beta_{1\text{-}40}$ reaction mixtures containing monomer, soluble aggregates, and fibril were formed at low salt concentrations (2–5 mmol/L) and shorter incubation times (4–5 h) and used within 1 h of preparation. Soluble $A\beta_{1\text{-}40}$ aggregates within these reaction mixtures were separated from fibril via centrifugation and from unreacted monomer via SEC on Superdex 75. Isolated soluble aggregates were used for experimentation within 1 h of purification. $A\beta_{1\text{-}40}$ fibrils, for which formation was optimized using high salt concentrations (150–250 mmol/L) and longer incubation times (15–20 h), were isolated via centrifugation (15 min, 18,000x*g*), resuspended in 40 mmol/L Tris-HCl (pH 8.0), and stored at 4°C for up to 1 week.

Determination of aggregate size

As described previously (Gonzalez-Velasquez and Moss 2008), aggregate size was assessed via hydrodynamic radius (R_H) measurements using a DynaPro MSX DLS instrument (Wyatt Technology, Santa Barbara, CA) to assimilate auto-correlated light intensity data for calculation of translational diffusion coefficients that could be converted to R_H using the Stokes-Einstein equation. Values of R_H are reported as the intensity-weighted mean R_H derived from the predominant peak of the regularized histogram (using Dynamics software by Wyatt Technology). Isolated soluble $A\beta_{1\text{-}40}$ aggregates consistently exhibited R_H ranging between 25 and 100 nm, and unpurified $A\beta_{1\text{-}40}$ reaction mixtures exhibited R_H ranging from 25 to 500 nm.

Cell culture and treatment

Endothelial monolayers were composed of ACBRI 376 primary HBMVECs (Cell Systems, Kirkland, WA) isolated from normal human brain cortex via elutriation. This cell model was employed previously to study $A\beta_{1\text{-}40}$ activation of endothelium for monocyte adhesion and transmigration (Gonzalez-Velasquez and Moss 2008). Cells were purchased at passage 2, grown on surfaces coated with CS-C Attachment Factor, and sustained in CS-C Complete Medium containing penicillin (100 Units/mL) and streptomycin (100 μg/mL) at 37°C in a humid atmosphere of 5% CO_2 and 95% air. HBMVECs were used for experimentation between passages 4 and 8.

HBMVEC monolayers were prepared for experiments as described previously (Gonzalez-Velasquez and Moss 2008). Briefly, endothelial cells were seeded at a density of 5×10^5–6×10^5 cells/mL onto a cell culture surface coated with 2.0% gelatin containing 100 μg/mL collagen: 22×22 mm glass coverslips (Costar, Corning Inc, Acton, MA) for immunocytochemistry or 6.5 mm diameter polycarbonate membrane inserts (0.4 μm pore size, 1×10^8 pores/cm^2) (Costar, Corning Inc., Acton, MA) assembled into 24-well plates for permeability assays and TEER measurements. HBMVEC monolayers were sustained until confluence (5–6 days, 37 °C, 5% CO_2) in CS-C Serum Free Medium containing penicillin (100 Units/mL) and streptomycin (100 μg/mL) and supplemented with hydrocortisone (550

nmol/L) to promote barrier properties (Weidenfeller *et al.* 2005). Resulting confluent cell monolayers exhibited TEER values (~550 Ω/cm^2) similar to those reported for other BBB models (Deli *et al.* 2005) (Supplemental material Fig. S1a). In addition, the localization of ZO-1 staining at cell borders confirmed the presence of TJ complexes characteristic of endothelial cells of the BBB (Kniesel and Wolburg 2000; Ballabh *et al.* 2004; Forster 2008), and the absence of immunocytochemical staining for muscle α-actin, a protein expressed by vascular smooth muscle cells, demonstrated the purity of the HBMVEC cultures (Supplemental material Fig. S1b).

Confluent monolayers were treated with $A\beta_{1\text{-}40}$ preparations (isolated monomer, isolated soluble aggregates, resuspended fibril, or an unpurified reaction mixture containing monomer, soluble aggregates, and fibril) diluted into CS-C Serum Free Medium containing hydrocortisone to achieve final concentrations of 0.1–10 μmol/L. Parallel treatment with an equivalent dilution of buffer in media served as a negative control, while monolayers treated with 10 Units/well TNF-α served as a positive control.

Permeability assay

Permeability assays were performed following $A\beta_{1\text{-}40}$, negative control, or positive TNF-α control treatment for 24 h (37°C, 5% CO_2). After activation, monolayers were washed and their barrier function determined by adding 100 μL of 50 μg/mL FITC-BSA in CS-C Serum Free Medium to the apical (top) chamber and replenishing 600 μL cell culture medium in the basolateral (bottom) chamber to ensure equal osmotic pressure across the monolayer. Albumin was selected for permeability determinations because it is the principal plasma protein and is involved in maintaining transendothelial oncotic pressure. Albumin is adequately large to ensure that its transendothelial transport across intact monolayers is greatly restricted and strongly influenced by the formation of large paracellular openings within the endothelial monolayer (McAmis *et al.* 2003; Mehta and Malik 2006).

Transport of FITC-BSA across the monolayer was allowed to proceed for 25 h (37 °C, 5% CO_2). Permeated FITC-BSA was quantified at 0.5–1 h time intervals by removing 50 μL aliquots from the basolateral chamber and assessing fluorescence of permeated FITC-BSA using a BioTek Synergy 2 microplate reader (Winooski, VT) equipped with an excitation filter of 485±10 nm and an emission filter of 535±12.5 nm and implementing baseline (CS-C Serum Free Medium) subtraction. 50 μL of fresh media was added to the basolateral chamber after each reading to eliminate convective transport that could result from hydrostatic pressure gradients across the monolayer. Fluorescence measured at each time point was corrected for the resulting dilution. FITC-BSA concentrations in the basolateral chamber, $[BSA]_{basolateral}$, were determined from a calibration curve of the fluorescence signal, which was linearly dependent upon the BSA concentration.

Permeability, P, was calculated according to a linear approximation of Fick's Law:

$$PS = \frac{J}{[BSA]_{0,apical} - [BSA]_{0,basolateral}} \quad (1)$$

where S is the surface area of the transwell insert and $[BSA]_{0,\ apical}$ and $[BSA]_{0,\ basolateral}$ are the initial concentrations of FITC-BSA in the top and bottom chambers, respectively. The flux, J, was calculated as the product of the volume of the basolateral chamber times the rate of increase in basolateral FITC-BSA concentration determined from the linear region of $[BSA]_{basolateral}$ vs. time. Permeability was measured for negative control, positive control, and experimental treatments of endothelial monolayers, as well as for membrane supports in the absence of monolayers. Diffusional permeability coefficients (P_e) were then calculated by correction for the permeability of the membrane support in series with the monolayer:

$$\frac{1}{P_e S} = \frac{1}{P_{experimental} S} - \frac{1}{P_{insert} S} \quad (2)$$

Results are reported either as P_e or as relative P_e, the ratio of the P_e observed following $A\beta_{1\text{-}40}$ treatment to the P_e observed for untreated monolayers. Each treatment was performed in triplicate and values are reported as the mean ± SEM.

Transendothelial electrical resistance (TEER) measurements

TEER, which reflects the resistance to ion diffusion across the cell monolayer, was measured for HBMVEC monolayers both during the 5–6 day period required for monolayers to reach confluence and for 7 days following $A\beta_{1\text{-}40}$, negative control, or positive TNF-α control treatment. Measurements were acquired using sterilized electrodes connected to a voltohmmeter (Multicell-ERS, Millipore, Billerica, MA), whereby each of two electrodes was placed in the apical and basolateral chambers and the stable resistance reading was recorded. Resistance measurements were performed in triplicate and values of TEER are reported as the measured resistance per area of cell culture surface. TEER measurements are reported as the mean ± SEM.

Immunocytochemistry

Expression of the TJ-associated protein ZO-1 and the cytoskeleton protein α-actin were evaluated to verify, respectively, the integrity and purity of HBMVEC monolayers both at the onset of permeability assays and following $A\beta_{1\text{-}40}$, negative control, or positive TNF-α control treatment for 24 h (37°C, 5% CO_2). Treated and untreated HBMVEC monolayers were prepared for immunocytochemistry as described previously (Gonzalez-Velasquez and Moss 2008). Briefly, monolayers were washed with D-PBS, fixed (3.7% paraformaldehyde), permeabilized (0.1% Triton X-100, 0.01 mol/L glycine), and blocked (5% normal donkey serum, 1% BSA). Cells were incubated overnight at 4°C with the primary antibody, either rabbit polyclonal anti-ZO-1 antibody (1:50) or rabbit polyclonal anti-α-actin antibody (1:50). Monolayers were then blocked (5% normal donkey serum, 1% BSA) and bound primary antibody was detected with Cy3-conjugated donkey anti-rabbit secondary antibody (1:100). Monolayers were additionally stained with DAPI (1:5000). Samples were mounted in slides with DABCO solution for visualization under a Zeiss LSM confocal microscope (Carl Zeiss, Thornwood, NY) using a plan-apochromat 63X / 1.4 oil DIC immersion objective (Carl Zeiss). Images of at least ten different fields were acquired for each sample.

Micrographs were visualized and converted to TIFF documents using LSM 5 Image browser software and gamma adjusted using Adobe Photoshop 7.0.

Statistical analysis

Statistical analysis was performed with a one-way ANOVA using GraphPad Prism 5 software (San Diego, CA). When results from ANOVA analyses were significant, a test for linear trend assessed the dose-dependence or Dunnett's test for multiple comparisons identified groups with means significantly different from the control. Groups identified by Dunnett's test were further assessed using a two-tailed t-test to account for variations in scatter and define the level of significance. Reported levels of statistical significance are those observed using the test for linear trend or the two-tailed t-test. $P < 0.05$ was considered significant.

Results

Treatment of HBMVEC monolayers with $A\beta_{1\text{-}40}$ increases permeability

Permeability of confluent HBMVEC monolayers was assessed via transendothelial transport of FITC-BSA. A linear increase in the concentration of FITC-BSA transferred from the apical to the basolateral side of confluent HBMVEC monolayers was observed over the first 7 h, followed by deceleration towards equilibrium (Fig. 1a, insert). Values of P_e were calculated from an approximation of Fick's Law using early time points within the linear range as described in the Materials and methods. P_e for confluent HBMVEC monolayers fell between 1.1×10^{-5} and 3.6×10^{-5} cm/s, which is within the range expected for intact BBB models (Deli *et al.* 2005).

To assess the ability of $A\beta_{1\text{-}40}$ to promote permeability in HBMVEC monolayers, transendothelial transport of FITC-BSA was measured following 24 h treatment of monolayers with an unpurified $A\beta_{1\text{-}40}$ reaction mixture containing monomer, soluble aggregates, and fibril at a concentration of 5 μmol/L. This $A\beta_{1\text{-}40}$ treatment time and concentration was shown previously to be sub-toxic, as HBMVEC toxicity requires $A\beta_{1\text{-}40}$ concentrations greater than 10 μmol/L or treatment times exceeding 7 days (Gonzalez-Velasquez and Moss 2008). Transendothelial FITC-BSA transport across $A\beta_{1\text{-}40}$ stimulated monolayers occurred at a faster rate than did transport across untreated control monolayers; however, this increase was less pronounced than that observed for monolayers treated with TNF-α (Fig. 1a), a proinflammatory cytokine known to promote permeability of endothelial monolayers (Mehta and Malik 2006). Accordingly, a 2.6-fold increase in P_e was noted following HBMVEC monolayer exposure to an unpurified $A\beta_{1\text{-}40}$ reaction mixture, while TNF-α stimulation resulted in a 4.5-fold increase in P_e (Fig. 1b). Furthermore, $A\beta_{1\text{-}40}$-stimulated increases in endothelial monolayer permeability occurred in a dose-dependent manner as the concentration of the unpurified $A\beta_{1\text{-}40}$ reaction mixture was increased from 0.1 to 10 μmol/L (Fig. 2a). These results are in agreement with previous studies which have observed a dose-dependent increase in endothelial permeability following $A\beta_{25\text{-}35}$ treatment of porcine pulmonary artery endothelial cells (Blanc *et al.* 1997) and $A\beta_{1\text{-}40}$ treatment of bovine brain capillary endothelial cells (Strazielle *et al.* 2000) and extend these observations to a human brain endothelial cell model.

Changes in P_e were paralleled by changes in TEER. When confluent HBMVEC monolayers exhibiting a plateau in TEER (7 days) were exposed to an unpurified $A\beta_{1-40}$ reaction mixture, a linear decrease in TEER was observed when cultures were further maintained over a period of 7 days. The rate of this decline increased as the $A\beta_{1-40}$ concentration was increased from 2.5 to 10 μmol/L (Fig. 2b). A similar, although more pronounced, decline in TEER was observed following endothelial monolayer treatment with TNF-α, in agreement with reports by others that decreased TEER values accompany increases in permeability resulting from cytokine treatment (Deli *et al.* 2005). Together, these results demonstrate that $A\beta_{1-40}$ is capable of inducing a dose-dependent increase in permeability of HBMVEC monolayers. Furthermore, the correlation between solute transport, which is dependent upon the sum of all changes in junctional pathways, and TEER, which reflects changes in the pathway of lowest resistance between cells, supports the opening of paracellular pathways following $A\beta_{1-40}$ treatment.

Treatment of HBMVEC monolayers with $A\beta_{1-40}$ induces re-localization of TJ-associated protein ZO-1

To examine whether $A\beta_{1-40}$ induced changes in endothelial monolayer permeability are accompanied by changes in endothelial TJs, expression patterns for the TJ-associated protein ZO-1 were examined. Untreated HBMVEC monolayers displayed a continuous ZO-1 staining pattern localized along intracellular borders where it is involved in TJ complexes characteristic of BBB endothelial cells (Fig. 3b). Nuclear staining of ZO-1 was also observed, as has been reported previously for epithelial cells (Gottardi *et al.* 1996). When monolayers were exposed to 5 μmol/L of an unpurified $A\beta_{1-40}$ reaction mixture containing monomer, soluble aggregates, and fibril, a discontinuous staining pattern at the cell borders was accompanied by an increase of ZO-1 expression in the cytoplasm (Fig. 3e). This change in expression pattern was similar to that observed following exposure of monolayers to the cytokine TNF-α (Fig. 3c), known to alter ZO-1 expression in corneal epithelial cells (Kimura *et al.* 2008), intestinal epithelial cells (Ma *et al.* 2004), and kidney epithelial cells (Soler *et al.* 1999). In addition, nuclear ZO-1 staining was augmented (Fig. 3e), consistent with the documented role for ZO-1 in signal transduction events induced by the loss of cell-cell contacts (Balda and Matter 2000). Re-location of ZO-1 occurred in a dose-dependent manner when monolayers were incubated with increasing concentrations of the unpurified $A\beta_{1-40}$ reaction mixture (2.5, 5.0, and 10.0 μmol/L) (Figs. 3d–f). These results compliment observations in other studies illustrating that $A\beta_{1-42}$ is capable of stimulating translocation of TJ proteins claudin-5 and ZO-2 from the cell surface to the cytoplasm in microvascular endothelial cells isolated from rat brain (Marco and Skaper 2006) and extend these observations by incorporating both a different Aβ isoform and a human brain endothelial cell model to demonstrate changes in a novel TJ protein. These findings also confirm that $A\beta_{1-40}$-induced increases in HBMVEC monolayer permeability result from the disruption of endothelial TJs.

Soluble $A\beta_{1-40}$ aggregates selectively increase endothelial monolayer permeability

Previously, we reported that only soluble $A\beta_{1-40}$ aggregation intermediates but not $A\beta_{1-40}$ monomer or mature fibril were capable of activating HBMVEC monolayers for increased adhesion and subsequent transmigration of monocyte cells (Gonzalez-Velasquez and Moss

2008). To similarly elucidate the species within the unpurified $A\beta_{1-40}$ reaction mixture responsible for enhancing monolayer permeability, values of P_e for HBMVEC monolayers treated with the unpurified $A\beta_{1-40}$ reaction mixture were compared to those observed following treatment with SEC-isolated monomer, resuspended fibril, or soluble aggregates depleted of mature fibrils via centrifugation and resolved from unreacted monomer via SEC.

Treatment of HBMVEC monolayers with $A\beta_{1-40}$ monomer or fibril at concentrations as high as 10 μmol/L failed to alter endothelial monolayer permeability, while unpurified $A\beta_{1-40}$ reaction mixtures containing soluble aggregation intermediates increased P_e by 2.6-fold and 3.3-fold when monolayers were treated, respectively, at concentrations of 5 and 10 μmol/L (Fig. 4a). In contrast, HBMVEC monolayers treated with 1 or 2 μmol/L SEC-isolated soluble $A\beta_{1-40}$ aggregates exhibited a significant increase in P_e (Fig. 5a). A similar increase in P_e was observed when monolayers were treated with the same concentrations of an unpurified $A\beta_{1-40}$ reaction mixture which also contained soluble aggregates. As for HBMVEC monolayers treated with the unpurified $A\beta_{1-40}$ reaction mixture, dose-dependent increases in permeability were observed as the concentration of SEC-isolated soluble $A\beta_{1-40}$ aggregates was increased from 0.1 to 2 μmol/L (Fig. 5b). Changes in permeability induced by SEC-isolated soluble aggregates were similar in magnitude to those observed following treatment with the unpurified $A\beta_{1-40}$ reaction mixture over the range of concentrations studied.

Again, changes in P_e were paralleled by changes in TEER. The linear decrease observed in TEER following HBMVEC monolayer treatment with the $A\beta_{1-40}$ reaction mixture containing soluble aggregation intermediates was not evidenced when treatment was performed with SEC-isolated $A\beta_{1-40}$ monomer or resuspended $A\beta_{1-40}$ fibril (Fig. 4b). Together, these results confirm that unaggregated $A\beta_{1-40}$ monomer is inert and further indicate that the presence of aggregated $A\beta_{1-40}$ alone is insufficient to stimulate changes in endothelium that lead to enhanced monolayer permeability. Instead, soluble $A\beta_{1-40}$ aggregation intermediates appear to be primarily responsible for inducing increases in endothelial monolayer permeability.

$A\beta_{1-40}$ stimulated increases in endothelial permeability correlate inversely with aggregate size

In addition to demonstrating previously that soluble $A\beta_{1-40}$ aggregation intermediates are primarily responsible for endothelial activation, we reported that smaller soluble aggregates of $A\beta_{1-40}$ exhibited the most pronounced stimulation of HBMVEC monolayers for monocyte adhesion (Gonzalez-Velasquez and Moss 2008). To determine whether $A\beta_{1-40}$-induced increases in endothelial monolayer permeability also exhibit a similar dependence upon aggregate size, transendothelial FITC-BSA transport was assessed following treatment of HBMVEC monolayers with 5 μmol/L unpurified $A\beta_{1-40}$ reaction mixtures which displayed average R_H ranging from 25–120 nm. As shown in Fig. 6, physiological activity exhibited an inverse relationship with aggregate size. Endothelial permeability was increased by less than 35% following monolayer treatment with soluble $A\beta_{1-40}$ aggregates exhibiting R_H near 120 nm. However, $A\beta_{1-40}$ stimulation of permeability rose steadily as aggregate size decreased until P_e reached almost a 3-fold increase over untreated control

monolayers for aggregate preparations exhibiting R_H of 25–35 nm. These results demonstrate that, as for activation of endothelial monolayers for adhesion, small soluble $A\beta_{1\text{-}40}$ aggregates are also the most potent activators of increases in endothelial permeability.

Discussion

In CAA associated with AD, an age-related accumulation of fibrillar Aβ is observed within perivascular drainage pathways and in close proximity to the abluminal surface of the arterial and capillary endothelium (Kalaria 1992; Rensink *et al.* 2003; Kumar-Singh 2008; Weller *et al.* 2008). Stiffening of vessels associated with age and vascular disease reduces arterial pulsations that drive perivascular drainage, and age-associated changes in basement membrane composition and conformation have been speculated to contribute to protein deposition. Blockage of perivascular drainage pathways by deposited Aβ further promotes the development of CAA (Weller *et al.* 2008). This progressive accumulation of cerebrovascular Aβ culminates in hemorrhagic stroke and is preceded by disruption of the BBB. Studies in both animals (Jancso *et al.* 1998; Su *et al.* 1999; Farkas *et al.* 2003; Dickstein *et al.* 2006) and cell culture (Blanc *et al.* 1997; Strazielle *et al.* 2000; Marco and Skaper 2006) have confirmed the ability of Aβ to compromise BBB integrity; however, the responsible Aβ species has not yet been explored. Soluble Aβ aggregates play a role in neuronal dysfunction associated with AD via inhibition of long-term potentiation (LTP) (Kirkitadze *et al.* 2002; Barghorn *et al.* 2005; Klyubin *et al.* 2005; Townsend *et al.* 2006; Walsh and Selkoe 2007), stimulation of tau hyperphosphorylation (De Felice *et al.* 2007), induction of synaptic loss (Shankar *et al.* 2007), disruption of complex learned behavior (Cleary *et al.* 2005; Lesne *et al.* 2006), and initiation of neurotoxicity (reviewed in Kirkitadze *et al.* 2002; Walsh and Selkoe 2007). Furthermore, our lab has recently confirmed that small, soluble $A\beta_{1\text{-}40}$ aggregates selectively activate BBB endothelial monolayers for increased adhesion and subsequent transmigration of monocyte cells (Gonzalez-Velasquez and Moss 2008). In this study, we provide evidence that small soluble $A\beta_{1\text{-}40}$ aggregates are also primarily responsible for promoting permeability in monolayers of HBMVECs via disruption of endothelial TJs.

Other studies have provided evidence that sub-toxic concentrations of Aβ can induce dose-dependent increases in endothelial monolayer permeability. Aged preparations of $A\beta_{25\text{-}35}$ stimulated albumin permeability in monolayers formed by porcine pulmonary artery endothelial cells (Blanc *et al.* 1997), while freshly solubilized preparations of $A\beta_{1\text{-}40}$ stimulated polyethylene glycol permeability in monolayers formed by bovine brain capillary endothelial cells (Strazielle*et al.* 2000). In the current study, $A\beta_{1\text{-}40}$ monomer isolated via SEC and mature $A\beta_{1\text{-}40}$ fibril isolated via centrifugation failed to elicit any change in the permeability of HBMVEC monolayers (Fig. 4); however, sub-toxic concentrations of SEC-isolated soluble $A\beta_{1\text{-}40}$ aggregates increased permeability in a dose-dependent manner (Fig. 5). By characterizing unpurified $A\beta_{1\text{-}40}$ reaction mixtures containing soluble aggregation intermediates using DLS, it was further demonstrated that $A\beta_{1\text{-}40}$ preparations exhibiting smaller average R_H elicited a more pronounced increase in endothelial monolayer permeability (Fig. 6). These results suggest that small soluble aggregates present in $A\beta_{1\text{-}40}$ preparations are primarily responsible for stimulating permeability in endothelial

monolayers. In other studies, $A\beta_{1-40}$ or $A\beta_{25-35}$ concentrations of 5 μmol/L or greater were required to observe endothelial monolayer permeability increases, while the current results demonstrate that significant increases in diffusional permeability coefficients were observed for both unpurified $A\beta_{1-40}$ reaction mixtures and SEC-isolated soluble $A\beta_{1-40}$ aggregates at concentrations as low as 500 nmol/L (Fig. 5). These differences may be attributed to a significant quantity of monomer or mature fibril, respectively, in freshly dissolved $A\beta_{1-40}$ and aged $A\beta_{25-35}$ preparations.

The free exchange of plasma proteins across BBB endothelial monolayers is restricted by the presence of endothelial TJs. The paracellular barrier formed by these structures is maintained by homotypic recognition of integral membrane proteins, including claudins, occludin, and junction-associated adhesion molecules, that are bound to ZO cytoplasmic proteins which link TJs to the cell cytoskeleton (Kniesel and Wolburg 2000; Ballabh *et al.* 2004; Forster 2008). In the current study, observed changes in endothelial monolayer permeability were accompanied by re-localization of the TJ-associated protein ZO-1 (Fig. 3) as well as decreases in TEER (Figs. 2 and 4), a measure of the resistance to ion diffusion across the cell monolayer. These results provide evidence that $A\beta_{1-40}$-stimulated increases in monolayer permeability result from a disruption of endothelial TJs and increased paracellular transport. A similar correlation among increased permeability, reorganization of TJ proteins, and decreased TEER has also been applied to demonstrate increased transport via paracellular pathways following the treatment of rat brain microvascular endothelial cells with the permeability-inducing compound bradykinin (Liu *et al.* 2008), the exposure of bovine brain microvascular endothelial cells to ZO toxin (Karyekar *et al.* 2003), and the incubation of the basolateral surface of bovine brain microvascular endothelial cells in the presence of serum-containing media (Colgan *et al.* 2008). Conversely, decreased endothelial monolayer permeability following exposure of HBMVECs to shear (Siddharthan *et al.* 2007) and treatment of rat brain microvascular endothelial cells with the vasodialator adrenomedullin (Honda *et al.* 2006) has been correlated with increased expression of TJ proteins and elevated TEER. The observed $A\beta_{1-40}$-induced changes in cellular relocalization of ZO-1 are also in agreement with previous studies which have demonstrated changes in the cellular distribution of TJ proteins claudin-5 and ZO-2 following treatment of rat brain microvessel endothelial cells with a freshly solubilized preparation of $A\beta_{1-42}$ (Marco and Skaper 2006). However, in this study changes in protein distribution were observed only following incubation with higher $A\beta_{1-42}$ concentrations of 20 μmol/L. These differences may be attributed to a lower concentration of small soluble aggregation intermediates relative to $A\beta_{1-40}$ preparations used in the current study or to the use of a different isoform of Aβ.

Aβ-induced compromise of the BBB has the potential to contribute to the progressive pathology of AD. Increases in BBB permeability permit the entry of blood-borne xenobiotics and endogenous molecules into the brain, disturbing CNS homeostasis and promoting neuronal dysfunction and death. For example, serum albumin is capable of inducing degeneration of cholinergic neurons (Moser and Humpel 2007), while serum IgG is known to initiate neutorphil infiltration and associated immune response in the brain (Kadota *et al.* 2000). A weakened BBB, in conjunction with Aβ activation of

cerebrovascular endothelium for adhesion (Gonzalez-Velasquez and Moss 2008), can additionally facilitate entry of peripheral immune cells into the brain that activate microglia and perpetuate immune response (Farkas *et al.* 2003). Some blood-borne substances that enter the brain as a result of BBB leakage or microhemmorhage may also serve as a nidus for Aβ deposition, as suggested by the association of serum proteins with amyloid plaques (Kalaria *et al.* 1991; Akiyama *et al.* 1992; Kimura *et al.* 1994; Perlmutter *et al.* 1995; Wisniewski *et al.* 1997) and the close proximity of plaques to the microvasculature (Kalaria 1992; Kumar-Singh *et al.* 2005; Stone 2008). These vessel-associated plaques are observed to associate with dystrophic neurites in the surrounding neuropil (Kumar-Singh *et al.* 2005). Alternatively, increases in BBB permeability oppose polarized transendothelial transport systems which facilitate brain-to-blood efflux of certain compounds. These transport systems include ATP-binding cassette transporters that selectively eliminate neurotoxic compounds from the brain (Zheng *et al.* 2003; Zlokovic 2005) and K^+-ATPase which maintains a low K^+ concentration within the brain to regulate its effect on transmission of nerve impulses (Zheng *et al.* 2003). A number of researchers have hypothesized that BBB leakage may be an early event in AD pathogenesis (Kalaria 1992; Rhodin and Thomas 2001; Zlokovic 2005; Zipser *et al.* 2007). This speculation contributes to what has been more formally set forth as the neurovascular hypothesis of AD, which proposes that vascular dysfunction leads to BBB compromise and chemical alterations in the neuronal milieu that ultimately result in neuronal dysfunction and death (Zlokovic 2005). In particular, a role for the microvasculature is supported by the high incidence of association of amyloid plaques with cerebrovascular capillaries (Kalaria 1992; Kumar-Singh et al. 2005) and the positive correlation between severity of microvascular CAA and markers of AD progression (Attems and Jellinger 2004). Alternatively, others have suggested that Aβ deposition may be an adaptive response in which Aβ serves a protective role by functioning as an antioxidant (Berthon 2000; Lee *et al.* 2007), participating in the innate immune response (Campbell 2001), or retaining structural integrity at local sites of injury (Atwood *et al.* 1998). Cerebrovascular Aβ, specifically, has been speculated to serve as a vascular sealant (Atwood *et al.* 2003; Chaney *et al.* 2003).

Various isoforms and preparations of Aβ have been shown to induce a number of other responses in endothelium and vascular function that also have the potential to contribute to AD pathogenesis. Some of these responses may also be elicited primarily by small soluble $Aβ_{1-40}$ aggregates. In fact, we previously observed the same inverse correlation between aggregate size and physiological activity for $Aβ_{1-40}$ activation of HBMVEC monolayers as evidenced by an increase in the adhesion of monocyte cells (Gonzalez-Velasquez and Moss 2008). Although no other studies have specifically explored the role of soluble Aβ aggregates in endothelial biology and vascular function, some studies do suggest a role for these species. For example, when endothelial cell cultures were treated with freshly solubilized Aβ preparations, Aβ isoforms known to exhibit a high propensity for self-association, including $Aβ_{1-40}$ containing the Dutch E22Q mutation and $Aβ_{1-42}$, elicited a more pronounced response than did $Aβ_{1-40}$ in the promotion of inflammatory cytokine release (Suo *et al.* 1998), the prevention of angiogenesis (Paris *et al.* 2005), and the induction of endothelial toxicity (Miravalle *et al.* 2000; Folin *et al.* 2005). Similarly, at concentrations of freshly solubilized $Aβ_{1-40}$ or $Aβ_{1-42}$ below those required to modify

vasoconstriction, vasoconstriction could be enhanced only when $A\beta_{1-40}$ or $A\beta_{1-42}$ incubation occurred in the presence of oxidized low density lipoprotein to enhance assembly(Stanyer *et al.* 2004; Smith *et al.* 2007). Pre-aggregated fibrils, however, elicited no change in vasoconstriction (Smith *et al.* 2007). Similarly, prevention of angiogenesis could not be observed in the presence of pre-aggregated preparations of $A\beta_{1-40}$ or Dutch $A\beta_{1-40}$E22Q fibrils, and freshly solubilized preparations which prevented angiogenesis were observed to contain low molecular weight oligomers when analyzed by Western blotting (Paris *et al.* 2005). Each of these correlations suggests that the presence of small aggregates in freshly prepared Aβ solutions that have begun to undergo assembly are required to elicit changes in endothelial and vascular function.

Results from the current study establish the selective ability of soluble $A\beta_{1-40}$ aggregates to stimulate HBMVEC monolayers for increased permeability. Changes in permeability are accompanied by other indicators of BBB dysfunction, including a decrease in TEER and a re-localization of TJ proteins away from cell borders. Furthermore, an inverse correlation between aggregate size and diffusional permeability coefficients provides evidence that smaller soluble aggregates exhibit the most pronounced effect on endothelial monolayer permeability. These findings extend previous results which demonstrate that these same species are also primarily responsible for activation of HBMVEC monolayers for enhanced adhesion and subsequent transmigration of monocytes (Gonzalez-Velasquez and Moss 2008). Small soluble $A\beta_{1-40}$ aggregates may also elicit other changes in endothelium that have been speculated to contribute to neurodegeneration. Consequently, interactions between small soluble $A\beta_{1-40}$ aggregates and the endothelium may represent a viable point of therapeutic intervention for both CAA and AD.

Supplementary Material

Refer to Web version on PubMed Central for supplementary material.

Acknowledgments

We are grateful to Dr. Matthew Wolf and Dr. William McAmis (University of South Carolina School of Medicine) for their assistance with permeability assays and kind donation of transwell microplates. This work was supported by a Beginning Grant-In-Aid (0565387U) from the American Heart Association, Mid-Atlantic Affiliate to MAM. In addition, this publication was made possible in part by NIH Grant Number P20 RR-016461 from the National Center for Research Resources. Its contents are solely the responsibility of the authors and do not necessarily represent the official views of the NIH.

ABBREVIATIONS

Aβ	amyloid-β protein
ADDL	Aβ-derived diffusible ligand
AD	Alzheimer's disease
CAA	cerebral amyloid angiopathy
BBB	blood-brain barrier
BSA	bovine serum albumin

DABCO	1,4-diazabicyclo[2.2.2]octane
DAPI	4′,6′-diamidino-2-phenylindole dihydrochloride
D-PBS	Dulbecco's phosphate buffered saline
DLS	dynamic light scattering
FITC	fluorescein isothiocyanate
HBMVEC	human brain microvascular endothelial cells
LTP	long-term potentiation
P_e	diffusional permeability coefficient
R_H	hydrodynamic radius
SEC	size exclusion chromatography
TJ	tight junction
TEER	transendothelial electrical resistance
TNF-α	tumor necrosis factor-α
ZO-1	zonula occludin-1

References

Akiyama H, Ikeda K, Kondo H, McGeer PL. Thrombin accumulation in brains of patients with Alzheimer's disease. Neurosci Lett. 1992; 146:152–154. [PubMed: 1491781]

Attems J, Jellinger KA. Only cerebral capillary amyloid angiopathy correlates with Alzheimer pathology - a pilot study. Acta Neuropathol. 2004; 107:83–90. [PubMed: 14655019]

Atwood CS, Bowen RL, Smith MA, Perry G. Cerebrovascular requirement for sealant, anti-coagulant and remodeling molecules that allow for the maintenance of vascular integrity and blood supply. Brain Res Brain Res Rev. 2003; 43:164–178. [PubMed: 14499467]

Atwood CS, Moir RD, Huang X, Scarpa RC, Bacarra NM, Romano DM, Hartshorn MA, Tanzi RE, Bush AI. Dramatic aggregation of Alzheimer Aβ by Cu(II) is induced by conditions representing physiological acidosis. J Biol Chem. 1998; 273:12817–12826. [PubMed: 9582309]

Balda MS, Matter K. The tight junction protein ZO-1 and an interacting transcription factor regulate ErbB-2 expression. EMBO J. 2000; 19:2024–2033. [PubMed: 10790369]

Ballabh P, Braun A, Nedergaard M. The blood-brain barrier: an overview: structure, regulation, and clinical implications. Neurobiol Dis. 2004; 16:1–13. [PubMed: 15207256]

Barghorn S, Nimmrich V, Striebinger A, et al. Globular amyloid β-peptide oligomer - a homogenous and stable neuropathological protein in Alzheimer's disease. J Neurochem. 2005; 95:834–847. [PubMed: 16135089]

Berthon G. Does human βA4 exert a protective function against oxidative stress in Alzheimer's disease? Med Hypotheses. 2000; 54:672–677. [PubMed: 10859663]

Blanc EM, Toborek M, Mark RJ, Hennig B, Mattson MP. Amyloid β-peptide induces cell monolayer albumin permeability, impairs glucose transport, and induces apoptosis in vascular endothelial cells. J Neurochem. 1997; 68:1870–1881. [PubMed: 9109512]

Campbell A. β-amyloid: friend or foe. Med Hypotheses. 2001; 56:388–391. [PubMed: 11359367]

Chaney MO, Baudry J, Esh C, Childress J, Luehrs DC, Kokjohn TA, Roher AE. Aβ, aging, and Alzheimer's disease: a tale, models, and hypotheses. Neurol Res. 2003; 25:581–589. [PubMed: 14503011]

Claudio L. Ultrastructural features of the blood-brain barrier in biopsy tissue from Alzheimer's disease patients. Acta Neuropathol. 1996; 91:6–14. [PubMed: 8773140]

Cleary JP, Walsh DM, Hofmeister JJ, Shankar GM, Kuskowski MA, Selkoe DJ, Ashe KH. Natural oligomers of the amyloid-β protein specifically disrupt cognitive function. Nat Neurosci. 2005; 8:79–84. [PubMed: 15608634]

Colgan OC, Collins NT, Ferguson G, Murphy RP, Birney YA, Cahill PA, Cummins PM. Influence of basolateral condition on the regulation of brain microvascular endothelial tight junction properties and barrier function. Brain Res. 2008; 1193:84–92. [PubMed: 18177846]

De Felice FG, Wu D, Lambert MP, et al. Alzheimer's disease-type neuronal tau hyperphosphorylation induced by Aβ oligomers. Neurobiol Aging. 200710.1016/j.neurobiolaginig.2007.02.029

Deli MA, Abraham CS, Kataoka Y, Niwa M. Permeability studies on *in vitro* blood-brain barrier models: physiology, pathology, and pharmacology. Cell Mol Neurobiol. 2005; 25:59–127. [PubMed: 15962509]

Dickstein DL, Biron KE, Ujiie M, Pfeifer CG, Jeffries AR, Jefferies WA. Aβ peptide immunization restores blood-brain barrier integrity in Alzheimer disease. FASEB J. 2006; 20:426–433. [PubMed: 16507760]

Farkas IG, Czigner A, Farkas E, Dobo E, Soos K, Penke B, Endresz V, Mihaly A. Beta-amyloid peptide-induced blood-brain barrier disruption facilitates T-cell entry into the rat brain. Acta Histochem. 2003; 105:115–125. [PubMed: 12831163]

Folin M, Baiguera S, Tommasini M, Guidolin D, Conconi MT, De Carlo E, Nussdorfer GG, Parnigotto PP. Effects of β-amyloid on rat neuromicrovascular endothelial cells cultured *in vitro*. Int J Mol Med. 2005; 15:929–935. [PubMed: 15870895]

Forster C. Tight junctions and the modulation of barrier function in disease. Histochem Cell Biol. 200810.1007/s00418-00008-00424-00419

Gonzalez-Velasquez FJ, Moss MA. Soluble aggregates of the amyloid-β protein activate endothelial monolayers for adhesion and subsequent transmigration of monocyte cells. J Neurochem. 2008; 104:500–513. [PubMed: 17953673]

Gottardi CJ, Arpin M, Fanning AS, Louvard D. The junction-associated protein, zonula occludens-1, localizes to the nucleus before the maturation and during the remodeling of cell-cell contacts. Proc Natl Acad Sci USA. 1996; 93:10779–11084. [PubMed: 8855257]

Honda M, Nakagawa S, Hayashi K, Kitagawa N, Tsutsumi K, Nagata I, Niwa M. Adrenomedullin improves the blood-brain barrier function through the expression of claudin-5. Cell Mol Neurobiol. 2006; 26:109–118. [PubMed: 16763778]

Jancso G, Domoki F, Santha P, et al. β-amyloid (1–42) peptide impairs blood-brain barrier function after intracarotid infusion in rats. Neurosci Lett. 1998; 253:139–141. [PubMed: 9774169]

Jellinger KA. Alzheimer disease and cerebrovascular pathology: An update. J Neural Transm. 2002; 109:813–836. [PubMed: 12111471]

Kadota E, Muramatsu Y, Nonaka K, Karasuno M, Nishi K, Dote K, Hashimoto S. Biological functions of extravasated serum IgG in rat brain. Acta Neurochir Suppl. 2000; 76:69–72. [PubMed: 11450094]

Kalaria RN. The blood-brain barrier and cerebral microcirculation in Alzheimer disease. Cerebrovasc Brain Metab Rev. 1992; 4:226–260. [PubMed: 1389957]

Kalaria RN, Golde TE, Cohen ML, Younkin SG. Serum amyloid P in Alzheimer's disease. Implications for dysfunction of the blood-brain barrier. Ann NY Acad Sci. 1991; 640:145–148. [PubMed: 1776732]

Karyekar CS, Fasano A, Raje S, Lu R, Dowling TC, Eddington ND. Zonula occludens toxin increases the permeability of molecular weight markers and chemotherapeutic agents across the bovine brain microvessel endothelial cells. J Pharm Sci. 2003; 92:414–423. [PubMed: 12532391]

Kimura K, Teranishi S, Fukuda K, Kawamoto K, Nishida T. Delayed disruption of barrier function in cultured human corneal epithelial cells induced by tumor necrosis factor-α in a manner dependent on NF-κB. Invest Ophthalmol Vis Sci. 2008; 49:565–571. [PubMed: 18235000]

Kimura M, Arai H, Takahashi T, Iwamoto N. Amyloid-P-component-likeimmunoreactivity in beta/A4-immunoreactive deposits in Alzheimer-type dementia brains. J Neurol. 1994; 241:170–174. [PubMed: 8164020]

Kirkitadze MD, Bitan G, Teplow DB. Paradigm shifts in Alzheimer's disease and other neurodegenerative disorders: The emerging role of oligomeric assemblies. J Neurosci Res. 2002; 69:567–577. [PubMed: 12210822]

Klyubin I, Walsh DM, Lemere CA, et al. Amyloid β protein immunotherapy neutralizes Aβ oligomers that disrupt synaptic plasticity *in vivo*. Nat Med. 2005; 11:556–561. [PubMed: 15834427]

Kniesel U, Wolburg H. Tight junctions of the blood-brain barrier. Cell Mol Neurobiol. 2000; 20:57–76. [PubMed: 10690502]

Kumar-Singh S. Cerebral amyloid angiopathy: pathogenetic mechanisms and link to dense amyloid plaques. Genes Brain Behav. 2008; 7(Suppl 1):67–82. [PubMed: 18184371]

Kumar-Singh S, Pirici D, McGowan E, Serneels S, Ceuterick C, Hardy J, Duff K, Dickson D, Van Broeckhoven C. Dense-core plaques in Tg2576 and PSAPP mouse models of Alzheimer's disease are centered on vessel walls. Am J Pathol. 2005; 167:527–543. [PubMed: 16049337]

Lee HG, Zhu X, Castellani RJ, Nunomura A, Perry G, Smith MA. Amyloid-β in Alzheimer disease: the null versus the alternate hypotheses. J Pharmacol Exp Ther. 2007; 321:823–829. [PubMed: 17229880]

Lesne S, Koh MT, Kotilinek L, Kayed R, Glabe CG, Yang A, Gallagher M, Ashe KH. A specific amyloid-β protein assembly in the brain impairs memory. Nature. 2006; 440:352–357. [PubMed: 16541076]

Liu LB, Xue YX, Liu YH, Wang YB. Bradykinin increases blood-tumor barrier permeability by down-regulating the expression levels of ZO-1, occludin, and claudin-5 and rearranging actin cytoskeleton. J Neurosci Res. 2008; 86:1153–1168. [PubMed: 18183615]

Ma TY, Iwamoto GK, Hoa NT, Akotia V, Pedram A, Boivin MA, Said HM. TNF-α-induced increase in intestinal epithelial tight junction permeability requires NF-κB activation. Am J Physiol Gastrointest Liver Physiol. 2004; 286:G367–376. [PubMed: 14766535]

Maia LF, Mackenzie IR, Feldman HH. Clinical phenotypes of cerebral amyloid angiopathy. J Neurol Sci. 2007; 257:23–30. [PubMed: 17341423]

Marco S, Skaper SD. Amyloid β-peptide(1–42) alters tight junction protein distribution and expression in brain microvessel endothelial cells. Neurosci Lett. 2006; 401:219–224. [PubMed: 16644119]

McAmis WC, Schaeffer RC Jr, Baynes JW, Wolf MB. Menadione causes endothelial barrier failure by a direct effect on intracellular thiols, independent of reactive oxidant production. Biochim Biophys Acta. 2003; 1641:43–53. [PubMed: 12788228]

Mehta D, Malik AB. Signaling mechanisms regulating endothelial permeability. Physiol Rev. 2006; 86:279–367. [PubMed: 16371600]

Miravalle L, Tokuda T, Chiarle R, Giaccone G, Bugiani O, Tagliavini F, Frangione B, Ghiso J. Substitutions at codon 22 of Alzheimer's Aβ peptide induce diverse conformational changes and apoptotic effects in human cerebral endothelial cells. J Biol Chem. 2000; 275:27110–27116. [PubMed: 10821838]

Moser KV, Humpel C. Blood-derived serum albumin contributes to neurodegeneration via astroglial stress fiber formation. Pharmacology. 2007; 80:286–292. [PubMed: 17671402]

Paris D, Ait-Ghezala G, Mathura VS, Patel N, Quadros A, Laporte V, Mullan M. Anti-angiogenic activity of the mutant Dutch Aβ peptide on human brain microvascular endothelial cells. Brain Res Mol Brain Res. 2005; 136:212–230. [PubMed: 15893605]

Perlmutter LS, Barron E, Myers M, Saperia D, Chui HC. Localization of amyloid P component in human brain: vascular staining patterns and association with Alzheimer's disease lesions. J Comp Neurol. 1995; 352:92–105. [PubMed: 7714241]

Rensink AA, de Waal RM, Kremer B, Verbeek MM. Pathogenesis of cerebral amyloid angiopathy. Brain Res Brain Res Rev. 2003; 43:207–223. [PubMed: 14572915]

Rhodin JA, Thomas T. A vascular connection to Alzheimer's disease. Microcirculation. 2001; 8:207–220. [PubMed: 11528529]

Shankar GM, Bloodgood BL, Townsend M, Walsh DM, Selkoe DJ, Sabatini BL. Natural oligomers of the Alzheimer amyloid-β protein induce reversible synapse loss by modulating an NMDA-type glutamate receptor-dependent signaling pathway. J Neurosci. 2007; 27:2866–2875. [PubMed: 17360908]

Siddharthan V, Kim YV, Liu S, Kim KS. Human astrocytes/astrocyte-conditioned medium and shear stress enhance the barrier properties of human brain microvascular endothelial cells. Brain Res. 2007; 1147:39–50. [PubMed: 17368578]

Smith CC, Stanyer L, Betteridge DJ, Cooper MB. Native and oxidized low-density lipoproteins modulate the vasoactive actions of soluble β-amyloid peptides in rat aorta. Clin Sci. 2007; 113:427–434. [PubMed: 17531005]

Soler AP, Marano CW, Bryans M, Miller RD, Garulacan LA, Mauldin SK, Stamato TD, Mullin JM. Activation of NF-κB is necessary for the restoration of the barrier function of an epithelium undergoing TNF-α-induced apoptosis. Eur J Cell Biol. 1999; 78:56–66. [PubMed: 10082424]

Stanyer L, Betteridge DJ, Smith CC. Potentiation of β-amyloid polymerisation by low-density lipoprotein enhances the peptide's vasoactivity. Biochim Biophys Acta. 2004; 1670:147–155. [PubMed: 14738998]

Stone J. What initiates the formation of senile plaques? The origin of Alzheimer-like dementias in capillary haemorrhages. Med Hypotheses. 200810.1016/j.mehy.2008.04.007

Strazielle N, Ghersi-Egea JF, Ghiso J, Dehouck MP, Frangione B, Patlak C, Fenstermacher J, Gorevic P. *In vitro* evidence that β-amyloid peptide 1–40 diffuses across the blood-brain barrier and affects its permeability. J Neuropathol Exp Neurol. 2000; 59:29–38. [PubMed: 10744033]

Su GC, Arendash GW, Kalaria RN, Bjugstad KB, Mullan M. Intravascular infusions of soluble β-amyloid compromise the blood-brain barrier, activate CNS glial cells and induce peripheral hemorrhage. Brain Res. 1999; 818:105–117. [PubMed: 9914443]

Suo Z, Tan J, Placzek A, Crawford F, Fang C, Mullan M. Alzheimer's β-amyloid peptides induce inflammatory cascade in human vascular cells: The roles of cytokines and CD40. Brain Res. 1998; 807:110–117. [PubMed: 9757011]

Townsend M, Shankar GM, Mehta T, Walsh DM, Selkoe DJ. Effects of secreted oligomers of amyloid β-protein on hippocampal synaptic plasticity: a potent role for trimers. J Physiol. 2006; 572:477–492. [PubMed: 16469784]

Ujiie M, Dickstein DL, Carlow DA, Jefferies WA. Blood-brain barrier permeability precedes senile plaque formation in an Alzheimer disease model. Microcirculation. 2003; 10:463–470. [PubMed: 14745459]

Vinters HV. Cerebral amyloid angiopathy. A critical review. Stroke. 1987; 18:311–324. [PubMed: 3551211]

Walsh DM, Selkoe DJ. Aβ Oligomers - a decade of discovery. J Neurochem. 2007; 101:1172–1184. [PubMed: 17286590]

Weidenfeller C, Schrot S, Zozulya A, Galla HJ. Murine brain capillary endothelial cells exhibit improved barrier properties under the influence of hydrocortisone. Brain Res. 2005; 1053:162–174. [PubMed: 16040011]

Weller RO, Subash M, Preston SD, Mazanti I, Carare RO. Perivascular drainage of amyloid-β peptides from the brain and its failure in cerebral amyloid angiopathy and Alzheimer's disease. Brain Pathol. 2008; 18:253–266. [PubMed: 18363936]

Wisniewski HM, Vorbrodt AW, Wegiel J. Amyloid angiopathy and blood-brain barrier changes in Alzheimer's disease. Ann NY Acad Sci. 1997; 826:161–172. [PubMed: 9329688]

Zheng W, Aschner M, Ghersi-Egea JF. Brain barrier systems: a new frontier in metal neurotoxicological research. Toxicol Appl Pharmacol. 2003; 192:1–11. [PubMed: 14554098]

Zipser BD, Johanson CE, Gonzalez L, Berzin TM, Tavares R, Hulette CM, Vitek MP, Hovanesian V, Stopa EG. Microvascular injury and blood-brain barrier leakage in Alzheimer's disease. Neurobiol Aging. 2007; 28:977–986. [PubMed: 16782234]

Zlokovic BV. Neurovascular mechanisms of Alzheimer's neurodegeneration. Trends Neurosci. 2005; 28:202–208. [PubMed: 15808355]

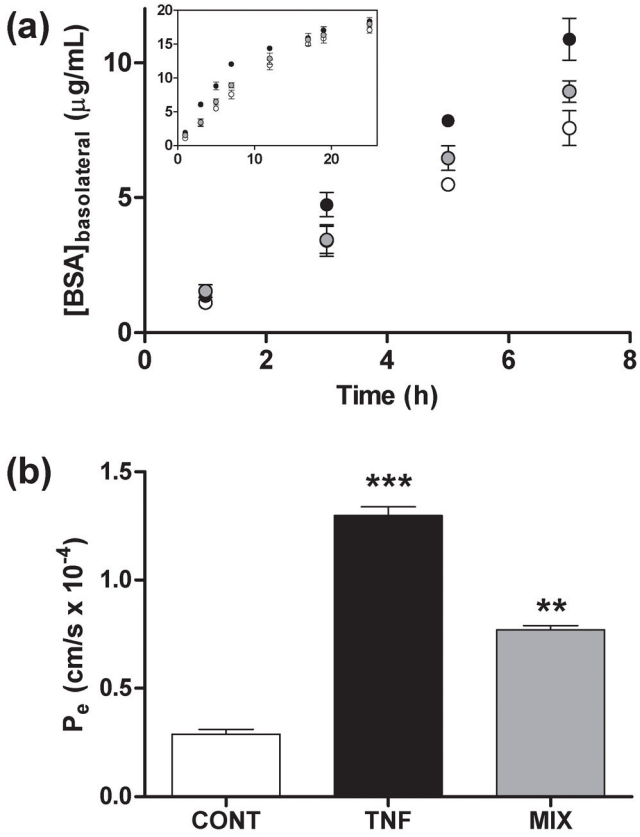

Fig. 1.

Effect of $A\beta_{1\text{-}40}$ aggregation mixtures on endothelial permeability in HBMVECs. HBMVEC monolayers grown to confluence on 6.5 mm diameter polycarbonate membrane inserts (0.4 μm pore size) were incubated for 24 h alone (○, CONT), with 10 Units TNF-α (●, TNF), or with 5 μmol/L unpurified $A\beta_{1\text{-}40}$ reaction mixture (R_H = 38 nm) (●, MIX). (a) Transfer of FITC-BSA from the apical to the basolateral chamber was monitored via fluorescence at 1, 3, 5, 7, 12, 15, 17, 19, and 25 h. (b) Diffusional permeability coefficients, P_e, were calculated from an approximation of Fick's Law and using the linear regression of $[\text{FITC-BSA}]_{basolateral}$ vs. time according to eq. 1 and eq. 2 as described under Materials and methods. *** $P < 0.001$; ** $P < 0.01$. All results are representative of at least five independent experiments performed with three repetitions. Error bars represent SEM.

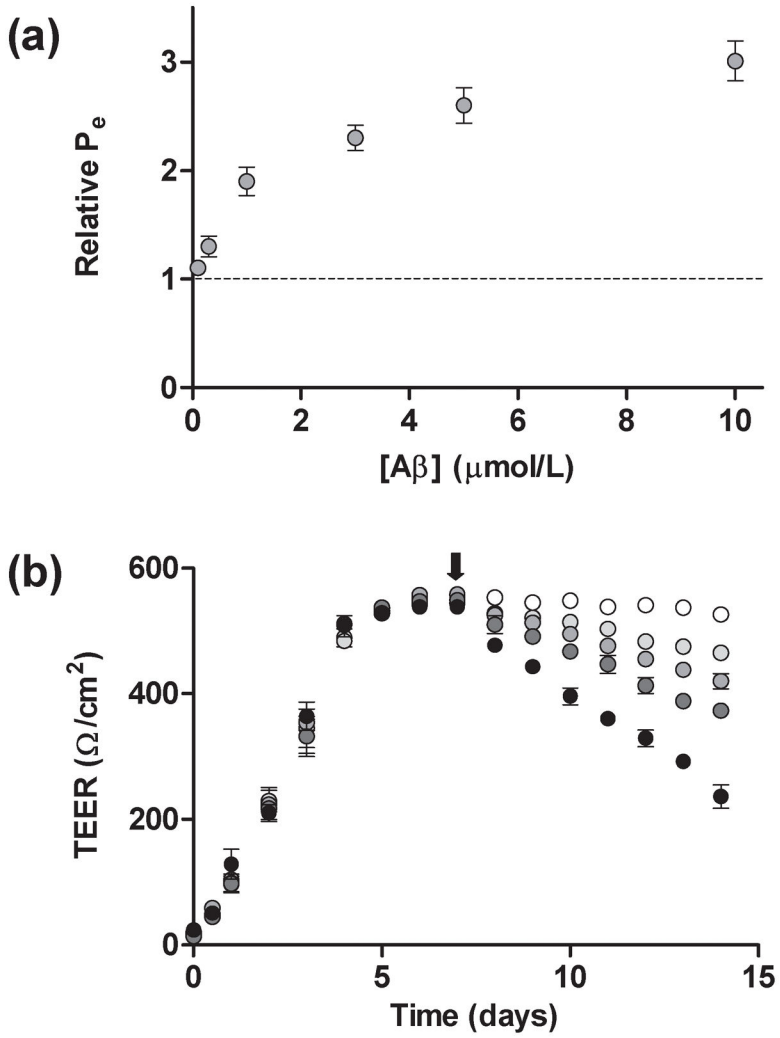

Fig. 2.

Dose-dependent effect of $A\beta_{1\text{-}40}$ aggregation mixtures on endothelial permeability and TEER in HBMVECs. (a) HBMVEC monolayers grown to confluence on 6.5 mm diameter polycarbonate membrane inserts (0.4 μm pore size) were stimulated via 24 h incubation. Confluent HBMVEC monolayers were incubated with 0, 0.1, 0.3, 1.0, 3.0, 5.0, or 10.0 μmol/L unpurified $A\beta_{1\text{-}40}$ reaction mixture (R_H = 65 nm). Values of P_e were calculated as in Fig. 1, and Relative P_e was determined as the ratio of the P_e observed following $A\beta_{1\text{-}40}$ activation to the P_e observed for untreated monolayers. Dependence of Relative P_e upon $A\beta_{1\text{-}40}$ concentration was significant ($P < 0.005$). Results are representative of at least three independent experiments, performed with three repetitions. Error bars represent SEM. (b) HBMVEC monolayers were grown on 6.5 mm diameter polycarbonate membrane inserts (0.4 μm pore size) in the presence of 550 nmol/L hydrocortisone, and TEER was measured following 0, 1, 2, 3, 4, 5, 6 and 7 days of growth as confluence was reached. At day 7 (arrow), confluent monolayers were incubated alone (○), with 10 Units TNF-α (●), or with 2.5 μmol/L ( ), 5.0 μmol/L ( ), or 10 μmol/L ( ) unpurified $A\beta_{1\text{-}40}$ reaction mixture. TEER was measured following 1, 2, 3, 4, 5, 6, and 7 days of incubation. Results are

representative of at least three independent experiments in which TEER measurements were performed with three repetitions. Error bars represent SEM. Some error bars lie within symbols.

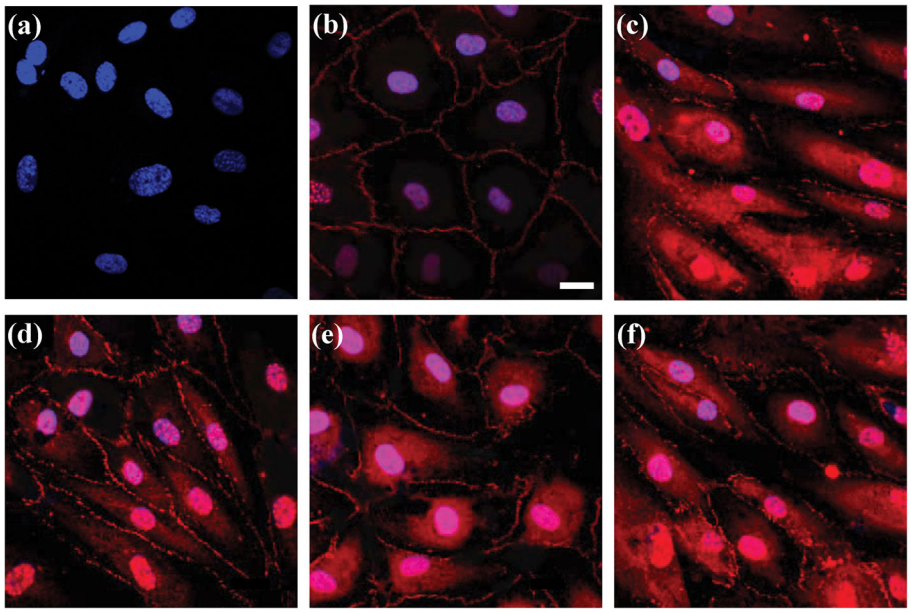

Fig. 3.

Effect of $A\beta_{1\text{-}40}$ aggregation mixtures on cellular localization of ZO-1 in HBMVECs. HBMVEC monolayers grown to confluence on glass coverslips were incubated for 24 h alone (panel b), with 10 Units TNF-α (panel c), or with 2.5, 5.0, or 10 μmol/L unpurified $A\beta_{1\text{-}40}$ reaction mixture (panels d, e, and f, respectively). Immunofluorescence staining was performed for TJ-associated protein ZO-1 (red) in conjunction with nuclear (DAPI) (blue) staining. Negligible background was observed in the absence of ZO-1 primary antibody (panel a). Images shown are representative of ten separate images acquired per sample. Images are shown relative to a scale bar of 20 μm.

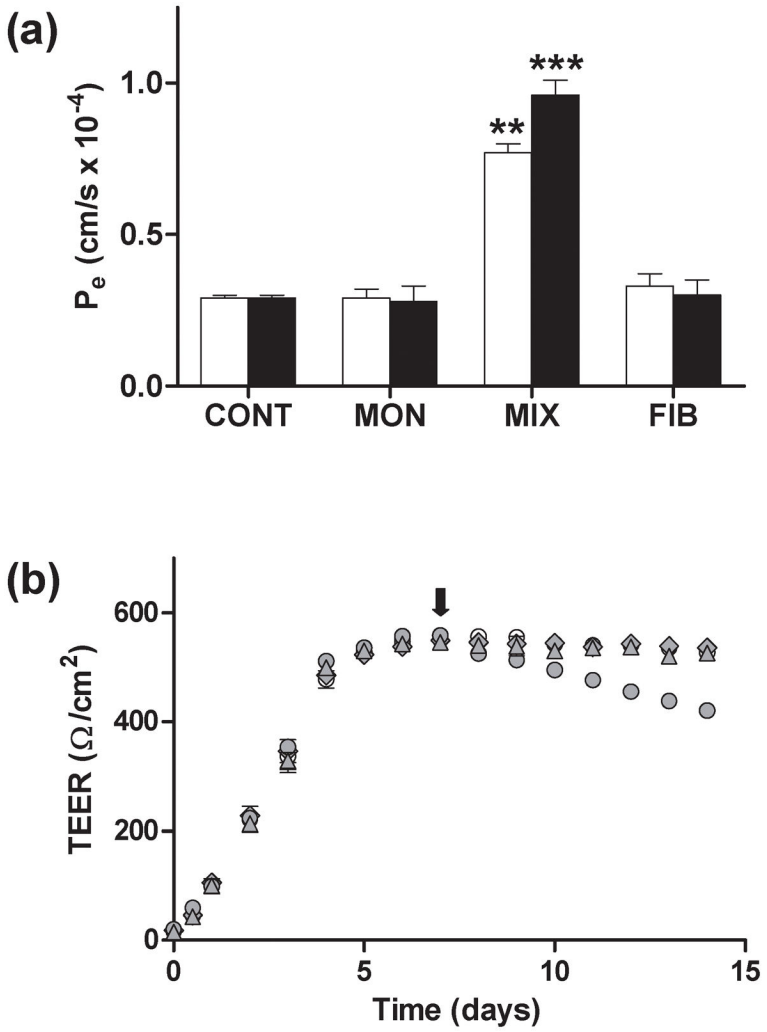

Fig. 4.

Comparison of the effect of $A\beta_{1\text{-}40}$ monomer, fibril, and aggregation mixtures on endothelial permeability in HBMVECs. (a) HBMVEC monolayers grown to confluence on 6.5 mm diameter polycarbonate membrane inserts (0.4 μm pore size) were stimulated via 24 h incubation. Confluent HBMVEC monolayers were incubated alone (CONT) or in the presence of SEC-isolated $A\beta_{1\text{-}40}$ monomer (MON), unpurified $A\beta_{1\text{-}40}$ reaction mixture (R_H = 65 nm) (MIX), or $A\beta_{1\text{-}40}$ fibril (FIB) isolated via centrifugation. $A\beta_{1\text{-}40}$ treatments were performed at concentrations of 5 μmol/L (open bars) or 10 μmol/L (closed bars). Values of P_e were calculated as in Fig. 1. *** $P < 0.001$, ** $P < 0.01$. (b) HBMVEC monolayers were grown on 6.5 mm diameter polycarbonate membrane inserts (0.4 μm pore size) in the presence of 550 nmol/L hydrocortisone, and TEER was measured following 0, 1, 2, 3, 4, 5, 6 and 7 days of growth as confluence was reached. At day 7 (arrow), confluent monolayers were incubated alone (○) or in the presence of 5 μmol/L SEC-isolated $A\beta_{1\text{-}40}$ monomer (◆), 5 μmol/L unpurified $A\beta_{1\text{-}40}$ reaction mixture (R_H = 65 nm) (●), or 5 μmol/L $A\beta_{1\text{-}40}$ fibril (▲) isolated via centrifugation. TEER was measured following 1, 2, 3, 4, 5, 6, and 7 days of incubation. Results are representative of at least three independent experiments in which

TEER measurements were performed with three repetitions. Error bars represent SEM. Some error bars lie within symbols.

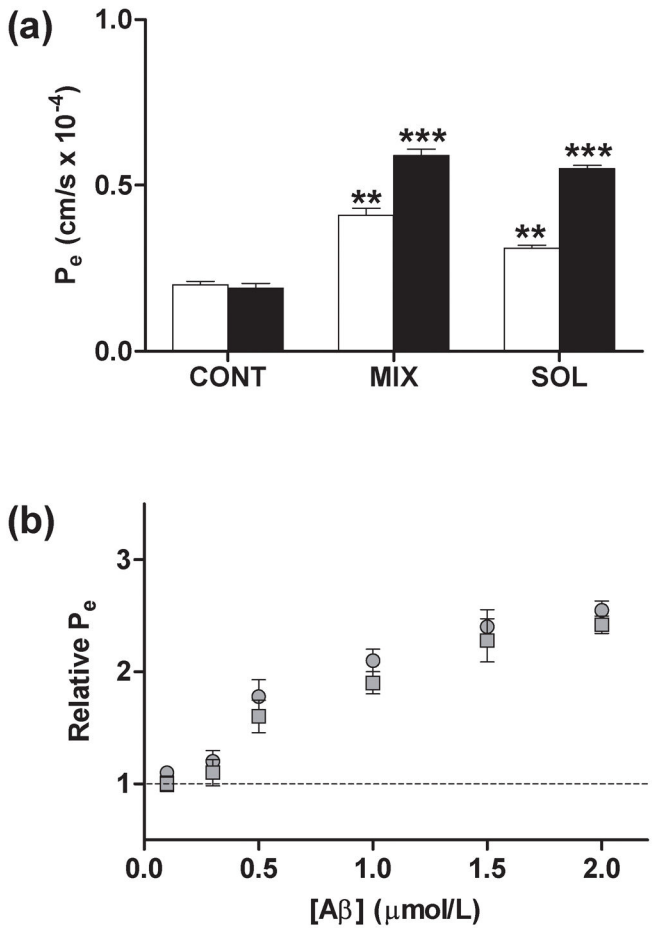

Fig. 5.

Effect of isolated soluble $A\beta_{1\text{-}40}$ aggregates on endothelial permeability in HBMVECs. HBMVEC monolayers grown to confluence on 6.5 mm diameter polycarbonate membrane inserts (0.4 μm pore size) were incubated for 24 h. (a) Confluent HBMVEC monolayers were incubated alone (CONT), with unpurified $A\beta_{1\text{-}40}$ reaction mixture (R_H = 63 nm) (MIX), or with SEC-isolated soluble $A\beta_{1\text{-}40}$ aggregates (R_H = 71 nm) (SOL). $A\beta_{1\text{-}40}$ treatments were performed at concentrations of 1 μmol/L (open bars) or 2 μmol/L (closed bars). Values for P_e were calculated as in Fig. 1. *** $P < 0.001$; ** $P < 0.01$. (b) Confluent HBMVEC monolayers were incubated with 0, 0.1, 0.3, 0.5, 1.0, 1.5, or 2.0 μmol/L unpurified $A\beta_{1\text{-}40}$ reaction mixture (R_H = 63 nm) (●) or SEC-isolated soluble $A\beta_{1\text{-}40}$ aggregates (R_H = 71 nm) (■). Relative P_e is reported as described in Fig. 2. Dependence of Relative P_e upon $A\beta_{1\text{-}40}$ treatment was significant for both the unpurified $A\beta_{1\text{-}40}$ reaction mixture ($P < 0.005$) and SEC-isolated soluble $A\beta_{1\text{-}40}$ aggregates ($P < 0.005$). All results are representative of at least three independent experiments, performed with three repetitions. Error bars represent SEM.

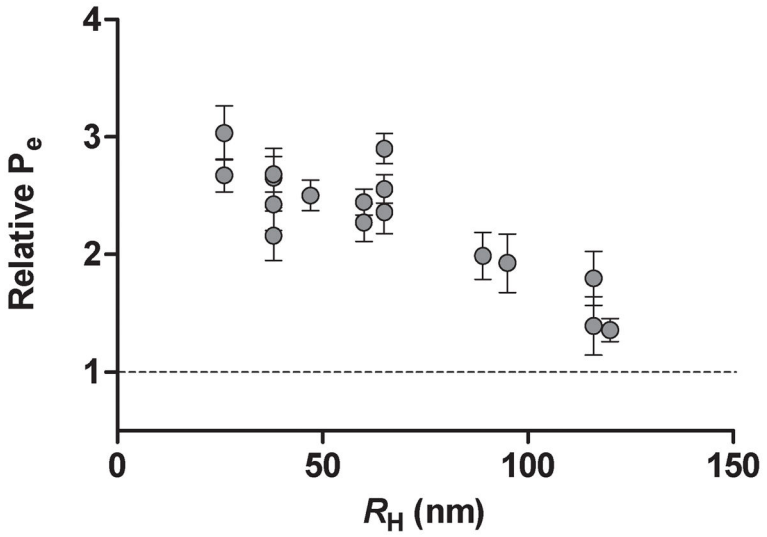

Fig. 6.

Effect of soluble $A\beta_{1\text{-}40}$ aggregate size on endothelial permeability in HBMVECs. Confluent HBMVEC monolayers were incubated for 24 h alone or with 5 μmol/L unpurified $A\beta_{1\text{-}40}$ reaction mixture for reaction mixtures that exhibited a range of R_H. Relative P_e is reported as described in Fig. 2. All results are performed with three repetitions. Error bars represent SEM.